

Modeling and simulation of isothermal reactive liquid chromatography for two component elution-effects of core-shell particles

Ugochukwu David Uche^{1*}, Mercy Uche², Folakemi Okafor³, Kate Utalor⁴

1-4 Department of Mathematics Programme, National Mathematical Centre Abuja, Nigeria

* Corresponding author: duj_uche@yahoo.com

Article Info

Received: 19 August 2022 Revised: 11 June 2022

Accepted: 15 June 2022 Available online: 30 August 2022

Abstract

In this work, semi-analytical solutions obtained by a combination of analytical and numerical procedure based on the numerical Hankel and Laplace transform inversions and solution of same model using high resolution finite volume numerical method are presented. These solutions are obtained for two-dimensional general rate models for isothermal liquid chromatographic reactors of cylindrical geometry packed with core-shell particles for an irreversible chemical reaction. This task is aimed at investigating the performance of the two-dimensional chromatography column under isothermal operating condition with the use of core-shell particles. The semi-analytical solutions are obtained considering the first-type and second-type boundary conditions. The use of core-shell particles is observed to produce less diffusive and sharper peaks but separation of chemical components is not significantly improved when compared with the results for porous particles.

Keywords: Liquid chromatography, general rate model, chemical reaction, semi-analytical solutions, numerical solutions.

MSC2010: 35K57; 65M08; 76M12; 76V05; 80A20

1 Introduction

Liquid chromatography is a separation technique that has been shown to be very useful in biochemical, fine chemicals, pharmaceutical, biological and food processing industries [1,2]. In reactive chromatography, conversion of reactants and components separation occur simultaneously within a chromatographic reactor and this process lead to production of products with high degree of purity [3]. The process has witnessed the development and application of different types and shapes of particles which are in various forms including fully porous, nonporous and core-shell particles [4-7].

Modeling the liquid chromatography process mathematically has largely contributed in the process development and improvement [1,2,8]. Several mathematical models have been used to describe the process of liquid chromatography. Most notable amongst them are the equilibrium

dispersive model (EDM), the lumped kinetic model (LKM) and the general rate model (GRM) and they range from the simplest to complex forms [1, 2, 9–11].

Linear one-dimensional (1D) and two-dimensional (2D) models of non-reactive and reactive chromatography have been solved by several authors [11–16]. In the current study, the analysis on two-dimensional general rate model (2D-GRM) studied in [17] for columns packed with fully porous particles is extended to the analysis of linear two-component reactive 2D-GRM considering columns packed with core-shell particles. Semi-analytical solutions of the model for irreversible reaction are derived for first-type (Dirichlet) and second-type (Danckwerts) boundary conditions by applying the Hankel transformation, Laplace transformation, eigen-decomposition technique and conventional solution technique for ordinary differential equations (ODEs) [18–20]. Numerical solutions are obtained by using high resolution finite volume scheme [21, 22] to the same model equations and are compared with the semi-analytical solution.

2 The governing equations

We consider an isothermal adsorption column filled with spherical particles of radius R_p . Let the time coordinate be denoted by t , let z represent the axial coordinate along the column length and let r represent the radial coordinate along the radius of the column. We assume that the injected solute travels along the column axis in the z -direction by convection and axial dispersion, while it spreads along the column radius by radial dispersion. Furthermore, we assume the following particular injection conditions in order to amplify the effects of mass transfer in the radial direction by introducing a new parameter \tilde{r} to split the inlet cross section of the column into an inner cylindrical zone and an outer annular ring or outer zone. Thus, there are three possible ways of sample injection into the column, these are through the inner zone, the outer zone, and through the whole cross-section. The latter case occurs if \tilde{r} is set equal to the radius of the column denoted by R_c . In the latter case, where no initial radial gradients are introduced into the column, the model equation becomes a simpler one-dimensional general rate model (1D-GRM) [23]. The classical mass balance equations for the liquid or mobile phase of adsorption in the column are given as

$$\frac{\partial c_1}{\partial t} + u \frac{\partial c_1}{\partial z} = D_{z,1} \frac{\partial^2 c_1}{\partial z^2} + D_{r,1} \left(\frac{\partial^2 c_1}{\partial r^2} + \frac{1}{r} \frac{\partial c_1}{\partial r} \right) - \frac{3}{R_p} F k_{\text{ext},1} (c_1 - c_{p,1}(r_p = R_p)), \quad (2.1)$$

$$\frac{\partial c_2}{\partial t} + u \frac{\partial c_2}{\partial z} = D_{z,2} \frac{\partial^2 c_2}{\partial z^2} + D_{r,2} \left(\frac{\partial^2 c_2}{\partial r^2} + \frac{1}{r} \frac{\partial c_2}{\partial r} \right) - \frac{3}{R_p} F k_{\text{ext},2} (c_2 - c_{p,2}(r_p = R_p)), \quad (2.2)$$

where for $i = 1, 2$, c_i is the concentration of i th component in the bulk of fluid, $c_{p,i}$ is the concentration of the same component in the particle pores, u is the interstitial velocity, $D_{z,i}$ is the axial dispersion coefficient of i th component, and $F = (1 - \epsilon)/\epsilon$ is the phase ratio with ϵ as the external porosity. Moreover, $D_{r,i}$ represents the radial dispersion coefficient and $k_{\text{ext},i}$ is the external mass transfer coefficient of i th component. Lastly, r_p denotes the radial coordinate of spherical particles of radius R_p .

For irreversible chemical reaction of the form ($A \rightarrow B$), the corresponding mass balance equations inside the particles pores are given as

$$\epsilon_p \frac{\partial c_{p,1}}{\partial t} + (1 - \epsilon_p) \frac{\partial q_{p,1}}{\partial t} = \frac{\epsilon_p D_{p,1}}{r_p^2} \frac{\partial}{\partial r_p} \left(r_p^2 \frac{\partial c_{p,1}}{\partial r_p} \right) - (1 - \epsilon_p) v_1 q_{p,1}, \quad (2.3)$$

$$\epsilon_p \frac{\partial c_{p,2}}{\partial t} + (1 - \epsilon_p) \frac{\partial q_{p,2}}{\partial t} = \frac{\epsilon_p D_{p,2}}{r_p^2} \frac{\partial}{\partial r_p} \left(r_p^2 \frac{\partial c_{p,2}}{\partial r_p} \right) - (1 - \epsilon_p) v_1 q_{p,1}, \quad (2.4)$$

where $D_{p,i}$ is the pore diffusivity of the i th component, ϵ_p is the internal porosity and v_1 is the reaction rate constant for component 1. The equilibrium linear adsorption isotherm is expressed as

$$q_{p,i} = a_i c_{p,i}, \quad i = 1, 2, \quad (2.5)$$

where a_i denotes the linear adsorption constant.

To further simplify the notations and reduce the number of variables, the following dimensionless variables are introduced:

$$\begin{aligned} x &= \frac{z}{L}, \quad \tau = \frac{ut}{L}, \quad \rho = \frac{r}{R_c}, \quad \rho_p = \frac{r_p}{R_p}, \quad Pe_{z,i} = \frac{Lu}{D_{z,i}}, \quad Pe_{\rho,i} = \frac{R_c^2 u}{D_{r,i} L} \\ \zeta_i &= \frac{k_{\text{ext}} R_p}{D_{p,i}}, \quad \eta_i = \frac{\epsilon_p D_{p,i} L}{R_p^2 u}, \quad \xi_i = 3\zeta_i \eta_i F, \quad \omega_i = \frac{L}{u} v_i. \end{aligned} \quad (2.6)$$

Here, L is the characteristic column length, $Pe_{z,i}$ and $Pe_{\rho,i}$ are the axial and radial peclet numbers, ζ_i is the mass transfer coefficient, ω_i is the dimensionless reaction rate constant of the i th component, η_i and ξ_i , are the dimensionless constants. Using the above dimensionless variables in Eqs. (2.1) to (2.2) for two components reaction (i.e $i = 1, 2$), we obtain

$$\frac{\partial c_1}{\partial \tau} + \frac{\partial c_1}{\partial x} = \frac{1}{Pe_{z_1}} \frac{\partial^2 c_1}{\partial x^2} + \frac{1}{Pe_{\rho_1}} \left(\frac{\partial^2 c_1}{\partial \rho^2} + \frac{1}{\rho} \frac{\partial c_1}{\partial \rho} \right) - \xi_1 [c_1 - c_{p,1}|_{\rho_p=1}], \quad (2.7)$$

$$\frac{\partial c_2}{\partial \tau} + \frac{\partial c_2}{\partial x} = \frac{1}{Pe_{z_2}} \frac{\partial^2 c_2}{\partial x^2} + \frac{1}{Pe_{\rho_2}} \left(\frac{\partial^2 c_2}{\partial \rho^2} + \frac{1}{\rho} \frac{\partial c_2}{\partial \rho} \right) - \xi_2 [c_2 - c_{p,2}|_{\rho_p=1}], \quad (2.8)$$

$$a_1^* \frac{\partial c_{p,1}}{\partial \tau} = \frac{\eta_1}{\rho_p^2} \frac{\partial}{\partial \rho_p} \left(\rho_p^2 \frac{\partial c_{p,1}}{\partial \rho_p} \right) - a_1(1 - \epsilon_p) \omega_1 c_{p,1}, \quad (2.9)$$

$$a_2^* \frac{\partial c_{p,2}}{\partial \tau} = \frac{\eta_2}{\rho_p^2} \frac{\partial}{\partial \rho_p} \left(\rho_p^2 \frac{\partial c_{p,2}}{\partial \rho_p} \right) + a_2(1 - \epsilon_p) \omega_1 c_{p,1}, \quad (2.10)$$

where $a_i^* = \epsilon_p + a_i(1 - \epsilon_p)$, $i = 1, 2$.

The above Eqs.(2.7)-(2.10) have been formulated for columns packed with fully porous particles. In order to study columns packed with core-shell particles, we follow the same procedure as suggested by [24]. Figure 1 shows a sketch of a spherical core-shell particle, with core radius fraction $\rho_{\text{core}} = R_{\text{core}}/R_p$. For fully porous particles ρ_p ranges from 0 to 1, while for core-shell particles it ranges

core-shell.eps
=200,1mm

Figure 1: Schematic diagram of a core-shell particle.

from $\rho_{\text{core}} = R_{\text{core}}/R_p$ to 1. Thus, for arbitrary core radius fraction $\rho_{\text{core}} \neq 0$, $\rho_{\text{core}} \leq \rho_p \leq 1$ for core-shell particles. While for fully porous particles, $\rho_{\text{core}}=0$. Hence we replace the ρ_p -axis by $0 \leq \gamma \leq 1$, where the dimensionless radial axis is

$$\gamma = \frac{\rho_p - \rho_{\text{core}}}{1 - \rho_{\text{core}}} \quad \Rightarrow \quad \rho_p = \gamma(1 - \rho_{\text{core}}) + \rho_{\text{core}}. \quad (2.11)$$

By substituting the above Eq.(2.11) into Eqs. (2.7)-(2.10), we now obtain the required governing equations for columns packed with core-shell particles given below as

$$\frac{\partial c_1}{\partial \tau} + \frac{\partial c_1}{\partial x} = \frac{1}{Pe_{z_1}} \frac{\partial^2 c_1}{\partial x^2} + \frac{1}{Pe_{\rho_1}} \left(\frac{\partial^2 c_1}{\partial \rho^2} + \frac{1}{\rho} \frac{\partial c_1}{\partial \rho} \right) - \xi_1 [c_1 - c_{p,1}|_{\gamma=1}], \quad (2.12)$$

$$\frac{\partial c_2}{\partial \tau} + \frac{\partial c_2}{\partial x} = \frac{1}{Pe_{z_2}} \frac{\partial^2 c_2}{\partial x^2} + \frac{1}{Pe_{\rho_2}} \left(\frac{\partial^2 c_2}{\partial \rho^2} + \frac{1}{\rho} \frac{\partial c_2}{\partial \rho} \right) - \xi_2 [c_2 - c_{p,2}|_{\gamma=1}], \quad (2.13)$$

$$(1 - \rho_{\text{core}})^2 a_1^* \frac{\partial c_{p,1}}{\partial \tau} = \eta_1 \left(\frac{\partial^2 c_{p,1}}{\partial \gamma^2} + \frac{2(1 - \rho_{\text{core}})}{(\gamma(1 - \rho_{\text{core}}) + \rho_{\text{core}})} \frac{\partial c_{p,1}}{\partial \gamma} \right) - a_1(1 - \epsilon_p) \omega_1 c_{p,1}, \quad (2.14)$$

$$(1 - \rho_{\text{core}})^2 a_2^* \frac{\partial c_{p,2}}{\partial \tau} = \eta_2 \left(\frac{\partial^2 c_{p,2}}{\partial \gamma^2} + \frac{2(1 - \rho_{\text{core}})}{(\gamma(1 - \rho_{\text{core}}) + \rho_{\text{core}})} \frac{\partial c_{p,2}}{\partial \gamma} \right) + a_2(1 - \epsilon_p) \omega_1 c_{p,1}. \quad (2.15)$$

The above equations have the following initial conditions:

$$c_i(\rho, x, 0) = 0, \quad 0 \leq x \leq 1, \quad 0 \leq \rho \leq 1, \quad (2.16)$$

$$c_{p,i}(\gamma, \rho, x, 0) = 0, \quad 0 \leq x \leq 1, \quad 0 \leq \rho \leq 1, \quad 0 \leq \gamma \leq 1. \quad (2.17)$$

Along the column radius, the following boundary conditions for Eqs. (2.12) and (2.13), considering the symmetry of radial profile and impermeability of the column wall, are used at $\rho = 0$ and $\rho = 1$:

$$\frac{\partial c_i(\rho = 0, x, \tau)}{\partial \rho} = 0, \quad \frac{\partial c_i(\rho = 1, x, \tau)}{\partial \rho} = 0, \quad i = 1, 2. \quad (2.18)$$

Also, the following boundary conditions are used for Eqs. (2.12) and (2.13), at both ends of the column for concentration pulses of finite width injected as Danckwerts inlet BCs:

For injection in the inner circular region, they are expressed as:

$$c_i(\rho, x = 0, \tau) - \frac{1}{Pe_{z,i}} \frac{\partial c_i(\rho, x = 0, \tau)}{\partial x} = \begin{cases} c_i^{\text{inj}}, & \text{if } 0 \leq \rho \leq \tilde{\rho} \text{ and } 0 \leq \tau \leq \tau_{\text{inj}}, \\ 0, & \tilde{\rho} < \rho \leq 1 \text{ or } \tau > \tau_{\text{inj}}. \end{cases} \quad (2.19)$$

While, for the injection through outer annular region, they are expressed as

$$c_i(\rho, x = 0, \tau) - \frac{1}{Pe_{z,i}} \frac{\partial c_i(\rho, x = 0, \tau)}{\partial x} = \begin{cases} c_i^{\text{inj}}, & \text{if } \tilde{\rho} < \rho \leq 1 \text{ and } 0 \leq \tau \leq \tau_{\text{inj}}, \\ 0, & 0 \leq \rho \leq \tilde{\rho} \text{ or } \tau > \tau_{\text{inj}}, \end{cases} \quad (2.20)$$

together with the Neumann conditions at the outlet of a finite length column

$$\left. \frac{\partial c_i(\rho, x, \tau)}{\partial x} \right|_{x=1} = 0, \quad i = 1, 2. \quad (2.21)$$

Here, c_i^{inj} is the inlet concentration of component i . The Danckwerts boundary condition tends to Dirichlet boundary conditions for large values of $Pe_{z,i}$.

For Eqs. (2.14) and (2.15), the boundary conditions at $\gamma = 0$ and $\gamma = 1$ are expressed as

$$\left. \frac{\partial c_{p,i}}{\partial \gamma} \right|_{\gamma=0} = 0, \quad \left. \frac{\partial c_{p,i}}{\partial \gamma} \right|_{\gamma=1} = (1 - \rho_{\text{core}}) \zeta_i (c_i - c_{p,i}|_{\gamma=1}), \quad i = 1, 2. \quad (2.22)$$

3 Semi-analytical solutions

The above chromatographic model along with associated initial and boundary conditions is analytically solved by successive implementation of the finite Hankel and Laplace transforms. The zeroth-order finite Hankel transform of $c_i(\rho, x, \tau)$ is defined as [18, 19]

$$c_{i,H}(\lambda_n, x, \tau) = H[c_i(\rho, x, \tau)] = \int_0^1 c_i(\rho, x, \tau) J_0(\lambda_n \rho) \rho d\rho. \quad (3.1)$$

The inverse Hankel transform is given as

$$c_i(\rho, x, \tau) = 2c_{i,H}(\lambda_n = 0, x, \tau) + 2 \sum_{n=1}^{\infty} c_{i,H}(\lambda_n, x, \tau) \frac{J_0(\lambda_n \rho)}{|J_0(\lambda_n)|^2}. \quad (3.2)$$

The Hankel transformation of Eqs. (2.12) and (2.13) with respect to coordinate ρ gives

$$\frac{\partial c_{i,H}}{\partial \tau} + \frac{\partial c_{i,H}}{\partial x} = \frac{1}{Pe_{z,i}} \frac{\partial^2 c_{i,H}}{\partial x^2} - \frac{\lambda_n^2}{Pe_{\rho,i}} c_{i,H} - \xi_i (c_{i,H} - c_{pi,H}|_{\gamma=1}). \quad (3.3)$$

Here, for $i = 1, 2$, $c_{i,H}(\lambda_n, x, \tau)$ and $c_{pi,H}(\lambda_n, x, \tau)$ are the zeroth-order finite Hankel transforms of $c_i(\rho, x, \tau)$ and $c_{p,i}(\gamma, \rho, x, \tau)$, respectively. The Laplace transformation of Hankel transformed function $c_{i,H}$ is defined as [19]

$$\bar{c}_{i,H}(\lambda_n, x, s) = \int_0^{\infty} e^{-st} c_{i,H}(\lambda_n, x, t) dt, \quad s \geq 0. \quad (3.4)$$

After applying the Laplace transformation on Eq. (3.3) with respect to τ and assuming that the initial concentration is zero, we get

$$\frac{1}{Pe_{z,i}} \frac{\partial^2 \bar{c}_{i,H}}{\partial x^2} - \frac{\partial \bar{c}_{i,H}}{\partial x} - \left(s + \frac{\lambda_n^2}{Pe_{\rho_i}} \right) \bar{c}_{i,H} - \xi_i (\bar{c}_{i,H} - \bar{c}_{pi,H}|_{\gamma=1}) = 0. \quad (3.5)$$

Here, $\bar{c}_{i,H}$ denotes the Hankel and Laplace transformed i -th concentration.

Applying the Laplace transform on Eqs. (2.14) and (2.15) and rearranging, we obtain

$$\frac{d^2}{d\gamma^2} [(\gamma(1 - \rho_{core}) + \rho_{core}) \bar{c}_{p,1}] - \left[\frac{a_1^* s + a_1 \omega_1 (1 - \epsilon_p)}{\eta_1} \right] (1 - \rho_{core})^2 [\gamma(1 - \rho_{core}) + \rho_{core}] \bar{c}_{p,1} = 0, \quad (3.6)$$

$$\begin{aligned} \frac{d^2}{d\gamma^2} [(\gamma(1 - \rho_{core}) + \rho_{core}) \bar{c}_{p,2}] - \frac{a_2^* s}{\eta_2} (1 - \rho_{core})^2 [\gamma(1 - \rho_{core}) + \rho_{core}] \bar{c}_{p,2} \\ + \frac{a_1 \omega_1 (1 - \epsilon_p)}{\eta_2} (1 - \rho_{core})^2 [\gamma(1 - \rho_{core}) + \rho_{core}] \bar{c}_{p,1} = 0. \end{aligned} \quad (3.7)$$

The general solution of Eq. (3.6) is given as:

$$\bar{c}_{p,1}(\gamma, \rho, x, s) = \frac{1}{[\gamma(1 - \rho_{core}) + \rho_{core}]} \left(A_1 e^{(1 - \rho_{core}) \sqrt{\alpha_1(s)} \gamma} + A_2 e^{-(1 - \rho_{core}) \sqrt{\alpha_1(s)} \gamma} \right), \quad (3.8)$$

where, $\alpha_1(s) = \frac{a_1^* s + a_1 (1 - \epsilon_p) \omega_1}{\eta_1}$. Here, A_1 and A_2 are the constants to be determined using the boundary conditions given in Eq. (2.22) which gives:

$$A_{1,2} = \pm \frac{\zeta_1 (\rho_{core} \sqrt{\alpha_1(s)} + 1) \bar{c}_1 / 2 \sinh(1 - \rho_{core})^2 (\sqrt{\alpha_1(s)})}{[(1 - \rho_{core})(\rho_{core} \alpha_1(s) - 1) + \zeta_1] + [(1 - \rho_{core})^2 + \rho_{core} \zeta_1] \sqrt{\alpha_1(s)} \coth((1 - \rho_{core}) \sqrt{\alpha_1(s)})}. \quad (3.9)$$

Thus, the solution in Eq. (3.8) at $\gamma = 1$, takes the form

$$\bar{c}_{p,1}|_{\gamma=1} = \bar{c}_1 f_1(s), \quad (3.10)$$

where

$$f_1(s) = \frac{\zeta_1 [\rho_{core} \sqrt{\alpha_1(s)} \coth(1 - \rho_{core}) (\sqrt{\alpha_1(s)} + 1)]}{[(1 - \rho_{core})(\rho_{core} \alpha_1(s) - 1) + \zeta_1] + [(1 - \rho_{core})^2 + \rho_{core} \zeta_1] \sqrt{\alpha_1(s)} \coth((1 - \rho_{core}) \sqrt{\alpha_1(s)})}. \quad (3.11)$$

Now using Eq. (3.10) in (3.7) and solving the resulting equation, we obtain

$$\bar{c}_{p,2}(\gamma, \rho, x, s) = \frac{1}{[\gamma(1 - \rho_{core}) + \rho_{core}]} \left(A_3 e^{(1 - \rho_{core}) \sqrt{\alpha_2(s)} \gamma} + A_4 e^{-(1 - \rho_{core}) \sqrt{\alpha_2(s)} \gamma} \right) + \frac{f_1(s) (1 - \epsilon_p) (1 - \rho_{core})^2 \omega_1 \bar{c}_1}{a_2^* s}, \quad (3.12)$$

where, $\alpha_2(s) = \frac{a_2^* s}{\eta_2}$. Applying the boundary conditions in Eq. (2.22) again and evaluating at $\gamma = 1$, we obtain:

$$\bar{c}_{p,2}|_{\gamma=1} = \bar{c}_2 f_2(s) + \bar{c}_1 g(s), \quad (3.13)$$

where

$$f_2(s) = \frac{\zeta_2 [\rho_{core} \sqrt{\alpha_2(s)} \coth(1 - \rho_{core}) (\sqrt{\alpha_2(s)} + 1)]}{[(1 - \rho_{core})(\rho_{core} \alpha_2(s) - 1) + \zeta_2] + [(1 - \rho_{core})^2 + \rho_{core} \zeta_2] \sqrt{\alpha_2(s)} \coth((1 - \rho_{core}) \sqrt{\alpha_2(s)})}. \quad (3.14)$$

and

$$g(s) = \frac{a_1(1 - \epsilon_p)(1 - \rho_{\text{core}})^2 \omega_1 f_1(s)}{a_2^* s} [1 - f_2(s)]. \quad (3.15)$$

Taking the Hankel transform of Eqs. (3.10) and (3.13) with respect to ρ , we get

$$(\bar{c}_{p,1})_H |_{\gamma=1} = \bar{c}_{1,H} f_1(s), \quad (3.16)$$

$$(\bar{c}_{p,2})_H |_{\gamma=1} = \bar{c}_{2,H} f_1(s) + \bar{c}_{1,H} g(s). \quad (3.17)$$

Putting Eqs. (3.16) and (3.17) in Eq. (3.5) for $i = 1, 2$, we obtain

$$\frac{d^2 \bar{c}_{1,H}}{dx^2} - Pe_{z_1} \frac{d\bar{c}_{1,H}}{dx} - Pe_{z_1} \phi_1(s, \lambda_n) \bar{c}_{1,H} = 0, \quad (3.18)$$

$$\frac{d^2 \bar{c}_{2,H}}{dx^2} - Pe_{z_2} \frac{d\bar{c}_{2,H}}{dx} - Pe_{z_2} \phi_2(s, \lambda_n) \bar{c}_{2,H} = Pe_{z_2} \xi_2 g(s) \bar{c}_{1,H}, \quad (3.19)$$

where

$$\phi_i(s, \lambda_n) = s + \frac{\lambda_n^2}{Pe_{\rho,i}} + \xi_i (1 - f_i(s)) \quad i = 1, 2. \quad (3.20)$$

We represent Eqs. (3.18) and (3.19) in matrix notation and we take $Pe_{z,i} = Pe_z, i=1,2$. Then, we obtain

$$\frac{d^2}{dx^2} \begin{pmatrix} \bar{c}_{1,H} \\ \bar{c}_{2,H} \end{pmatrix} - Pe_z \frac{d}{dx} \begin{pmatrix} \bar{c}_{1,H} \\ \bar{c}_{2,H} \end{pmatrix} - \begin{pmatrix} Pe_z \phi_1(s, \lambda_n) & 0 \\ -Pe_z \xi_2 g(s) & Pe_z \phi_2(s, \lambda_n) \end{pmatrix} \begin{pmatrix} \bar{c}_{1,H} \\ \bar{c}_{2,H} \end{pmatrix} = \begin{pmatrix} 0 \\ 0 \end{pmatrix}. \quad (3.21)$$

Now we decouple the system by applying the Eigen-decomposition technique. To proceed, we define the coefficient matrix A of the system as

$$A = \begin{pmatrix} Pe_z \phi_1(s, \lambda_n) & 0 \\ -Pe_z \xi_2 g(s) & Pe_z \phi_2(s, \lambda_n) \end{pmatrix}. \quad (3.22)$$

We decompose A into a diagonal matrix using a non-singular matrix B such that the columns of B are the eigenvectors of A . The eigenvalues are given as

$$\lambda_i = Pe_z \phi_i(s, \lambda_n) \quad i = 1, 2 \quad (3.23)$$

and the corresponding eigenvectors are expressed as

$$x_1 = \begin{bmatrix} 1 \\ \frac{-\xi_2 g(s)}{\phi_1(s, \lambda_n) - \phi_2(s, \lambda_n)} \end{bmatrix}, \quad x_2 = \begin{bmatrix} 0 \\ 1 \end{bmatrix}. \quad (3.24)$$

Based on the above eigenvalues, the transformation matrix B can be expressed as

$$B = \begin{pmatrix} 1 & 0 \\ \frac{-\xi_2 g(s)}{\phi_1(s, \lambda_n) - \phi_2(s, \lambda_n)} & 1 \end{pmatrix}. \quad (3.25)$$

Using the matrix B , we can formulate the following linear transformation

$$\begin{bmatrix} \bar{c}_{1,H} \\ \bar{c}_{2,H} \end{bmatrix} = \begin{pmatrix} 1 & 0 \\ \frac{-\xi_2 g(s)}{\phi_1(s, \lambda_n) - \phi_2(s, \lambda_n)} & 1 \end{pmatrix} \begin{bmatrix} \bar{b}_{1,H} \\ \bar{b}_{2,H} \end{bmatrix}. \quad (3.26)$$

Applying the above linear transformation on Eq. (3.21), we get

$$\frac{d^2}{dx^2} \begin{pmatrix} \bar{b}_{1,H} \\ \bar{b}_{2,H} \end{pmatrix} - Pe_z \frac{d}{dx} \begin{pmatrix} \bar{b}_{1,H} \\ \bar{b}_{2,H} \end{pmatrix} - \begin{pmatrix} \lambda_1 & 0 \\ 0 & \lambda_2 \end{pmatrix} \begin{pmatrix} \bar{b}_{1,H} \\ \bar{b}_{2,H} \end{pmatrix} = \begin{pmatrix} 0 \\ 0 \end{pmatrix}. \quad (3.27)$$

Eq. (3.27) represents a system of two independent ODEs with their explicit solutions given as

$$\begin{aligned}\bar{b}_{1,H}(\rho, x, s) &= C_1 e^{m_1 x} + C_2 e^{m_2 x}, \\ \bar{b}_{2,H}(\rho, x, s) &= D_1 e^{n_1 x} + D_2 e^{n_2 x}.\end{aligned}\quad (3.28)$$

where

$$m_{1,2} = \frac{1}{2} P e_z \pm \frac{1}{2} \sqrt{P e_z^2 - 4\phi_1(s, \lambda_n)}, \quad n_{1,2} = \frac{1}{2} P e_z \pm \frac{1}{2} \sqrt{P e_z^2 - 4\phi_2(s, \lambda_n)}. \quad (3.29)$$

In the above equations, upper sign is chosen for index 1 and lower sign is chosen for index 2. Next we use the inlet and outlet boundary conditions described in Eqs. (2.19) (or (2.20)) and (2.21) to obtain values for the constants of integration C_i and D_i , $i = 1, 2$. First we consider the case where $P e_z$ is large and $x = \infty$, which gives the Dirichlet inlet and outlet boundary conditions.

Thus, the Hankel transformations of Eqs. (2.19) (or for outer zone injection (2.20)) and (2.21), for Dirichlet inlet and outlet boundary conditions, are given as

$$c_{i,H}(\lambda_n, x = 0, \tau) = \begin{cases} c_i^{\text{inj}} F(\lambda_n), & \text{if } 0 \leq \tau \leq \tau_{\text{inj}}, \\ 0, & \text{if } \tau > \tau_{\text{inj}}, \end{cases} \quad (3.30)$$

$$\left. \frac{\partial c_{i,H}(\lambda_n, x, \tau)}{\partial x} \right|_{x=\infty} = 0, \quad i = 1, 2. \quad (3.31)$$

For injection at the inner zone, $F(\lambda_n)$ is given as

$$F(\lambda_n) = \begin{cases} \frac{\tilde{\rho}^2}{2}, & \text{if } \lambda_n = 0, \\ \frac{\tilde{\rho}}{\lambda_n} J_1(\lambda_n \tilde{\rho}), & \text{if } \lambda_n \neq 0, \end{cases} \quad (3.32)$$

while for injection at the outer annular zone, it becomes

$$F(\lambda_n) = \begin{cases} \left(\frac{1}{2} - \frac{\tilde{\rho}^2}{2} \right), & \text{if } \lambda_n = 0, \\ -\frac{\tilde{\rho}}{\lambda_n} J_1(\lambda_n \tilde{\rho}), & \text{if } \lambda_n \neq 0. \end{cases} \quad (3.33)$$

After applying the Laplace transformation on boundary conditions in Eqs. (3.30) and (3.31), we obtain

$$\bar{c}_{i,H}(\lambda_n, x, s) = c_i^{\text{inj}} \frac{F(\lambda_n)}{s} (1 - e^{-s\tau_{\text{inj}}}), \quad \left. \frac{\partial \bar{c}_{i,H}}{\partial x} \right|_{x=\infty} = 0, \quad i = 1, 2. \quad (3.34)$$

Applying the linear transformation on Eq. (3.34), we obtain

$$\bar{b}_{1,H}(\lambda_n, x, s) = c_1^{\text{inj}} \frac{F(\lambda_n)}{s} (1 - e^{-s\tau_{\text{inj}}}), \quad \left. \frac{\partial \bar{b}_{1,H}}{\partial x} \right|_{x=\infty} = 0, \quad (3.35)$$

$$\begin{aligned}\bar{b}_{2,H}(\lambda_n, x, s) &= c_2^{\text{inj}} \frac{F(\lambda_n)}{s} (1 - e^{-s\tau_{\text{inj}}}) + \frac{\xi_2 g(s)}{\phi_1(s, \lambda_n) - \phi_2(s, \lambda_n)} \bar{b}_{1,H} \\ \left. \frac{\partial \bar{b}_{2,H}}{\partial x} \right|_{x=\infty} &= 0.\end{aligned}\quad (3.36)$$

Using the above boundary conditions in Eq. (3.28), we derive

$$C_i = 0, \quad \frac{(1 - e^{-s\tau_{\text{inj}}})}{s} F(\lambda_n) c_1^{\text{inj}}, \quad (3.37)$$

$$D_i = 0, \quad \frac{(1 - e^{-s\tau_{\text{inj}}})}{s} F(\lambda_n) \left[c_2^{\text{inj}} + \frac{\xi_2 g(s)}{\phi_1(s, \lambda_n) - \phi_2(s, \lambda_n)} c_1^{\text{inj}} \right] \quad i = 1, 2. \quad (3.38)$$

By using the values of C_i and D_i , together with the transformation in Eq. (3.26), we obtain the results

$$\bar{c}_{1,H}(\lambda_n, x, s) = \frac{(1 - e^{-s\tau_{inj}})}{s} F(\lambda_n) c_1^{inj} e^{m_2 x}, \quad (3.39)$$

$$\begin{aligned} \bar{c}_{2,H}(\lambda_n, x, s) = & \frac{(1 - e^{-s\tau_{inj}})}{s} F(\lambda_n) c_1^{inj} \left[\frac{\xi_2 g(s)}{\phi_1(s, \lambda_n) - \phi_2(s, \lambda_n)} \right] (e^{n_2 x} - e^{m_2 x}) \\ & + \frac{(1 - e^{-s\tau_{inj}})}{s} F(\lambda_n) c_2^{inj} e^{n_2 x}. \end{aligned} \quad (3.40)$$

Analytical Laplace inversions of the above equations are not possible due to the complicated nature of the results. Therefore, numerical Hankel and Laplace inversions are used to get back solutions in actual time domain [20]. The numerical inversion procedures were implemented in Matlab software.

Next, we consider the much realistic Danckwerts boundary conditions case. The Hankel transformations of Eqs. (2.19), (or (2.20)) and (2.21) are given as

$$c_{i,H}(\lambda_n, x = 0, \tau) - \frac{1}{Pe_{z,i}} \frac{\partial c_{i,H}(\lambda_n, x = 0, \tau)}{\partial x} = \begin{cases} c_i^{inj} F(\lambda_n), & \text{if } 0 \leq \tau \leq \tau_{inj}, \\ 0, & \text{if } \tau > \tau_{inj}, \end{cases} \quad (3.41)$$

$$\left. \frac{\partial c_{i,H}(\lambda_n, x, \tau)}{\partial x} \right|_{x=1} = 0 \quad i = 1, 2. \quad (3.42)$$

Here, $F(\lambda_n)$ is given by Eq. (3.32) for the inner injection and by Eq. (3.33) for the outer annular injection.

After applying the Laplace transformation on these boundary conditions, we get

$$\bar{c}_{i,H}(\lambda_n, x = 0, s) - \frac{1}{Pe_{z,i}} \frac{\partial \bar{c}_{i,H}(\lambda_n, x = 0, s)}{\partial x} = \frac{c_i^{inj} F(\lambda_n)}{s} (1 - e^{-s\tau_{inj}}), \quad (3.43)$$

$$\left. \frac{\partial \bar{c}_{i,H}}{\partial x} \right|_{x=1} = 0. \quad (3.44)$$

Following the same solution procedure discussed above, we obtain the following results for Danckwerts BCs:

$$\bar{c}_{1,H}(\lambda_n, x, s) = \frac{[m_2 - m_1] e^{(m_1+m_2x)} \left[\frac{F(\lambda_n) c_1^{inj}}{s} (1 - e^{-s\tau_{inj}}) \right]}{m_2 e^{m_2} \left(1 - \frac{m_1}{Pe_z} \right) - m_1 e^{m_1} \left(1 - \frac{m_2}{Pe_z} \right)}, \quad (3.45)$$

$$\begin{aligned} \bar{c}_{2,H}(\lambda_n, x, s) = & \frac{[m_1 - m_2] e^{(m_1+m_2x)} \left[\frac{F(\lambda_n) c_1^{inj}}{s} (1 - e^{-s\tau_{inj}}) \right]}{m_2 e^{m_2} \left(1 - \frac{m_1}{Pe_z} \right) - m_1 e^{m_1} \left(1 - \frac{m_2}{Pe_z} \right)} \left[\frac{-\xi_2 g(s)}{\phi_1(s, \lambda_n) - \phi_2(s, \lambda_n)} \right] \\ & + \frac{(1 - e^{-s\tau_{inj}}) [n_1 - n_2] e^{(n_1+n_2x)} \left[c_2^{inj} + \frac{\xi_2 g(s) c_1^{inj}}{\phi_1(s, \lambda_n) - \phi_2(s, \lambda_n)} \right] F(\lambda_n)}{s \left[n_1 e^{n_1} \left(1 - \frac{n_2}{Pe_z} \right) - n_2 e^{n_2} \left(1 - \frac{n_1}{Pe_z} \right) \right]}. \end{aligned} \quad (3.46)$$

Again, no analytical Laplace inversions of the above equations are possible. Thus, numerical Laplace inversions are used to get back solutions in actual time domain [20].

4 Numerical case studies

Here, in order to test the correctness and to further get confidence on the obtained semi-analytical solutions, the semi discrete high resolution finite volume scheme (HR-FVS) of Koren is applied to numerically approximate the model equations [21, 22]. We also carry out several test cases to determine the performance and accuracy of the model. The parameters used for the simulation,

Table 1: Standard parameters used in the test problems.

Parameter	Symbol	Value
Length of column	L	8.0 cm
External porosity	ϵ_b	0.4
Internal porosity	ϵ_p	0.333
Interstitial velocity	u	2.0 cm/min
Axial dispersion coefficient	$D_z, (Pe_z)$	$2.6667 \times 10^{-2} \text{cm}^2/\text{min}, (600)$
Radial dispersion coefficient	$D_r, (Pe_r)$	$6.6667 \times 10^{-4} \text{cm}^2/\text{min}, (15)$
Henry's constant for component 1	a_1	2.5
Henry's constant for component 2	a_2	0.5
Dimensionless constant	η	2
Dimensionless constant	ζ	50

which are taken from the ranges typically found in high performance liquid chromatography (HPLC) applications, are given in Table 1. We have considered the case where only the reactant (component 1) is injected into the column, and it reacts depending on the coefficient of reaction to produce the product (component 2). Figure 2 (a) shows the effects of the reaction rate constant ω_1 for $\rho_{\text{core}} = 0.6$ and Figure 2 (b) shows the same reaction rate constant effects for $\rho_{\text{core}} = 0$. We see that in both



Figure 2: Inner zone injection: Effects of ω_1 on the concentration profiles for core-shell particles and fully porous particles.

results for core-shell particles and fully porous particles given in Figure 2, for the case where there is no reaction (i.e $\omega_1 = 0$), component 2 is not produced. We see also that for $\rho_{\text{core}} = 0.6$, the concentration profiles are narrower and less diffusive compared with the fully porous particles case for $\rho_{\text{core}} = 0$. It is observed also that in the cases where reaction occurs (i.e $\omega_1 \neq 0$), more product is produced in the case of fully porous particles as compared with that of the core-shell particles. Moreover, it is clear that in both cases, component 1 with a larger adsorption equilibrium constant elutes later from the column as compared to component 2 which has a smaller value of the adsorption equilibrium constant. Figure 3 shows the comparison of the analytical and numerical solutions. The numerical solutions were obtained by applying the suggested high-resolution finite



Figure 3: Inner zone injection: Comparison of analytical and numerical solutions.

volume scheme [21], for a mesh size of $60 \times 30 \times 10$ and was programmed in C language on a dual-core Intel processor laptop computer with a random access memory of 8 gigabytes. The numerical solutions are seen to show good agreements with the analytical solution, thereby increasing our confidence in the obtained analytical solutions. The effects of the axial dispersion coefficient Pe_z on the concentration profiles, obtained from the considered two types of boundary conditions are shown in Figure 4. For small axial dispersion coefficient $Pe_z = 10$, the solutions of both boundary

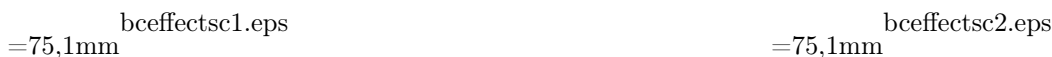


Figure 4: Inner zone injection: Effects of the axial Peclet number on the concentration profiles considering the two different boundary conditions.

conditions approach different values and the retention times also increase which in turn reduce the

column efficiency. Figure 5 illustrates the effects of the radial dispersion coefficient Pe_ρ on the concentration profiles. Both components were again injected just as in the previous considered cases and the injection was done from the inner zone. Figure 5 (a) shows that for small $Pe_\rho = 1.5$,



Figure 5: Inner zone injection: Effects of Pe_ρ on the concentration profiles.

there is no effect on the concentration profiles due to faster radial dispersion. The effects are clearly evident in Figure 5 (b) where the concentration profiles reduce at the middle of the column due to a slow moving radial dispersion for the considered $Pe_\rho = 150$. In Figure 6 (a), we see that slow



Figure 6: Inner and outer zone injections effects on the concentration profiles.

radial dispersion causes a large concentration profile at the inner region of the column for inner zone injection as compared to the case of outer zone injection shown in Figure 6 (b).

5 Conclusion

We have successfully solved two-dimensional linear model equations of reactive liquid chromatography for two components considering an irreversible reaction in a column packed with core-shell particles. The semi-analytical solutions were derived through a combined application of Hankel and Laplace transforms. The solutions were derived for first-type and second-type boundary conditions. A high-resolution finite volume scheme was used to numerically approximate the model equations and both the numerical solutions and the semi-analytical solutions were matched. From the results of our present study, the use of core-shell particles for small sample or diluted mixture in reactive chromatography provides no significant advantages over fully porous particles, for good column performance under isothermal conditions.

6 Competing Interests

The authors declare no competing financial interests.

7 Acknowledgement

The authors wish to thank the reviewers for their helpful suggestions which further improve this research work.

References

- [1] Guiochon G. Preparative liquid chromatography. *Journal of Chromatography A* **965**, 129-161 (2002).
- [2] Guiochon G., Felinger A., Shirazi D. G. & Katti A. M. Fundamentals of preparative and nonlinear chromatography, 2nd ed. *Elsevier Academic press, New York* (2006).
- [3] Agrawal G., Oh J., Sreedhar B., Tie S., Donaldson M. E., Frank T. C., Schultz A. K., Bommarius A. S. & Kawajiri Y. Optimization of reactive simulated moving bed systems with modulation of feed concentration for production of glycol ether ester. *Journal of Chromatography A* **1360**, 196-208 (2014).

- [4] Kirkland J. J., Truszkowski F. A., Dilks C. H. & Engel G. S. Superficially porous silica microspheres for fast high-performance liquid chromatography of macromolecules. *Journal of Chromatography A* **890**, 3-13 (2000).
- [5] Fekete S., Ganzler K. & Fekete, J. Facts and myths about columns packed with sub-3 μm and sub-2 μm particles. *Journal of Pharmaceutical and Biomedical Analysis* **51**, 56-64 (2010).
- [6] Rissler R. Separation of polyesters by gradient reversed-phase high- performance liquid chromatography on a 1.5 μm non-porous column. *Journal of Chromatography A* **871**, 243258 (2000).
- [7] Xiang Y. Q., Yan B. W., McNeff C. V., Carr P. W. & Lee M. L. Synthesis of micron diameter polybutadiene-encapsulated non-porous zirconia particles for ultrahigh pressure liquid chromatography. *Journal of Chromatography A* **1002**, 71-78 (2003).
- [8] Bellot J. C. & Condoretm J. S. Liquid Chromatography Modelling : A Review. *Process Biochemistry* **26**, 363-376 (1991).
- [9] Guiochon G. & Lin B. Modeling for preparative chromatography. *Academic Press* (2003).
- [10] Qamar S., Perveen S. & Seidel-Morgenstern A. Numerical approximation of a two-dimensional nonlinear and nonequilibrium model of reactive chromatography. *Industrial & Engineering Chemistry Research* **55**, 9003-9014 (2016).
- [11] Qamar S., Abbasi J., Mehwish A. & Seidel-Morgenstern A. Linear general rate model of chromatography for core-shell particles: Analytical solutions and moment analysis. *Chemical Engineering Science* **137**, 352-363 (2015).
- [12] Qamar S., Uche D. U., Khan F. U. & Seidel-Morgenstern A. Analysis of linear two-dimensional general rate model for chromatographic columns of cylindrical geometry. *Journal of Chromatography A* **1496**, 92-104 (2017).
- [13] Qamar S., Khan F. U., Mehmood Y. & Seidel-Morgenstern A. Analytical solution of a two-dimensional model of liquid chromatography including moment analysis. *Chemical Engineering Science* **116**, 576-589 (2014).
- [14] Qamar S., Bibi S., Khan F. U., Shah M., Javeed S. & Seidel-Morgenstern A. Irreversible and Reversible Reactions in a Liquid Chromatographic Column: Analytical Solutions and Moment Analysis. *Industrial & Engineering Chemistry Research* **53**, 2461-2472 (2014).
- [15] Bibi S., Qamar S. & Seidel-Morgenstern A. Irreversible and reversible reactive chromatography: Analytical solutions and moment analysis for rectangular pulse injections. *Journal of Chromatography A*. **1385**, 49-62 (2015).
- [16] Parveen S., Qamar S. & Seidel-Morgenstern A. Analysis of a two-Dimensional non-Equilibrium model of linear reactive Chromatography considering irreversible and reversible reactions. *Industrial & Engineering Chemistry Research* **55**, 2471-2482 (2015).
- [17] Uche U. D., Qamar S. & SeidelMorgenstern A. Analysis of two-dimensional models for liquid chromatographic reactors of cylindrical geometry. *International Journal of Chemical Kinetics* **51**, 563578 (2019).
- [18] Carslaw H. S. & Jaeger J. C. Operational methods in applied mathematics. *Oxford University Press, Oxford* (1953).
- [19] Sneddon I. H. The use of integral transforms. *McGraw-Hill, New York* (1972).
- [20] Durbin F. Numerical Inversion of Laplace Transforms: An efficient improvement to Dubner and Abate's Method. *The Computer Journal* **17**, 371-376 (1974).



- [21] Koren B. A robust upwind discretization method for advection, diffusion and source terms: *In C. B. Vreugdenhil, B. Koren, editors, Numerical Methods for Advection-Diffusion Problems, Volume 45 of Notes on Numerical Fluid Mechanics, chapter 5, pages 117-138, Vieweg Verlag, Braunschweig (1993).*
- [22] Javeed S., Qamar S., Seidel-Morgenstern A. & Warnecke G. Efficient and accurate numerical simulation of nonlinear chromatographic processes. *Journal of Computers & Chemical Engineering* **35**, 2294-2305 (2011).
- [23] Bashir S., Qamar S., Perveen S. & Seidel-Morgenstern A. Analysis of linear reactive general rate model of liquid chromatography considering irreversible and reversible reactions. *Chemical Engineering Research & Design* **119**, 140-159 (2017).
- [24] Gu T., Liu M., Cheng K. C., Ramaswamy S. & Wang C. A general rate model approach for the optimization of the core radius fraction for multicomponent isocratic elution in preparative nonlinear liquid chromatography using cored beads. *Chemical Engineering Science* **66**, 3531-3539 (2011).